

# Forward-angle incoherent photoproduction of pseudoscalar mesons off nuclei

T. E. Rodrigues<sup>1,\*</sup> and J. D. T. Arruda-Neto<sup>1,2</sup><sup>1</sup>*Physics Institute, University of São Paulo, P. O. Box 66318, CEP 05315-970, São Paulo, Brazil*<sup>2</sup>*FESP - São Paulo Engineering College, São Paulo, Brazil*

(Received 23 July 2012; published 10 September 2012)

The mechanism of forward angle incoherent photoproduction of pseudoscalar mesons off nuclei is revisited via the time-dependent multicolisional Monte Carlo (MCMC) intranuclear cascade model. Our results—combined with recent developments to address coherent photoproduction—reproduce with good accuracy recent JLab data of  $\pi^0$  photoproduction from carbon and lead at an average photon energy  $k \sim 5.2$  GeV. For the case of  $\eta$  photoproduction, our results for  $k = 9$  GeV suggest that future measurements to extract the  $\eta \rightarrow \gamma\gamma$  decay width via the Primakoff method should be focused on light nuclei, where the disentanglement between the Coulomb and strong amplitudes is more easily achieved. The prospects to use heavy nuclei data to access the unknown  $\eta N$  cross section in cold nuclear matter are also presented.

DOI: [10.1103/PhysRevC.86.037601](https://doi.org/10.1103/PhysRevC.86.037601)

PACS number(s): 25.20.Lj, 24.10.Lx, 12.40.Nn, 12.40.Vv

As first proposed by Primakoff [1], the electromagnetic coupling between real/virtual photons with the Coulomb field of atomic nuclei provides an appropriate framework for the extraction of the radiative decay widths of pseudoscalar mesons  $\Gamma_{P \rightarrow \gamma\gamma}$ . The angular distributions  $(\frac{d\sigma}{d\Omega})_{\gamma A \rightarrow PX}$  at extreme forward angles can be expressed as a sum of a coherent ( $X \equiv A$ ) and an incoherent part. The coherent contribution includes two different processes associated with the Coulomb ( $\gamma\gamma^*P$ ) and strong ( $\gamma VP$ ) couplings and can be evaluated under the context of the vector dominance model (VDM) using a Glauber multiple scattering calculation [2].

A further investigation of the mechanism of coherent photoproduction was recently proposed in Ref. [3]. In this work, the authors included initial and final state interactions (ISI/FSI) of the photoproduced mesons and calculated the Coulomb and strong components of the cross sections by constraining the relevant inputs with the elementary photoproduction off nucleons. Consequently the approach described in Ref. [3] opens the possibility to determine the relative strengths and phases between the Coulomb and strong components without free parameters.

The incoherent part includes the contributions from all nuclear excited states and can be factorized in terms of an incoherent sum of single nucleon amplitudes. As we have shown in recent works dedicated for incoherent  $\pi^0$  [4],  $\eta$  [5], and  $\omega$  [6] photoproduction, such inelastic mechanism can be well described in terms of semiclassical transport calculations, such as the multicolisional Monte Carlo (MCMC) intranuclear cascade model. A detailed explanation of the method can be found in Ref. [4] and references therein.

The radiative decay width of the neutral pion—which consists of a fundamental and measurable quantity of quantum chromodynamics (QCD)—has been subject of intense theoretical [7] and experimental efforts. From the experimental scenario, the most recent and high precision measurement was carried out by the PrimEx Collaboration at the Thomas Jefferson Laboratory (JLab) [8]. Detailed explanations regarding

the theoretical and experimental aspects of the radiative decay of pseudoscalar mesons can be found in Refs. [9,10].

In this Brief Report, we revisit the angular distributions of  $\pi^0$  and  $\eta$  photoproduction from complex nuclei at few GeV combining the state-of-the-art coupled-channel MCMC model with the recent predictions for coherent photoproduction obtained in Ref. [3]. Our goal is to provide a consistent interpretation for the cross section *excess* at larger angles found for  $\pi^0$  photoproduction in Ref. [3] when comparing their results with PrimEx data [8] and associate this difference to the mechanism of incoherent production; which was not taken into account in Ref. [3]. For the case of  $\eta$  photoproduction, we expect to show the potentialities of the MCMC model for the delineation of the inelastic background in future experiments dedicated for the chiral anomaly of QCD via the Primakoff method [11], and also the prospects to extract the in-medium  $\eta N$  cross section via nuclear measurements.

The nuclear incoherent (NI) cross section is calculated starting with the photoproduction mechanism off nucleons:

$$\gamma(k) + N(p_1) \rightarrow P(p) + N(p_2),$$

where  $k$  and  $p$  represent, respectively, the four-momentum of the incoming photon and produced meson, with  $p_1$  and  $p_2$  being the initial and final four-momentum of the struck nucleon. The second step describes the relativistic propagation of the mesons in the nuclear medium via the time-dependent semiclassical MCMC model. In this step, the nuclear effects of Fermi motion (FM), Pauli-blocking (PB), photon shadowing (PS), and meson-nucleus FSI are taken into account [4].

The nucleon cross sections for  $\pi^0$  and  $\eta$  photoproduction are calculated assuming a VDM and using a Regge phenomenology that includes  $\rho$  and  $\omega$  poles plus Regge cuts [12], such that [4,13,14]

$$\begin{aligned} \frac{d\sigma_N}{d\Omega} = & \frac{p_*^2}{32\pi^2} \left\{ \frac{F_3^2}{2m_N^2} - \left[ t + \left( \frac{\mu^2}{2k} \right)^2 \right] \left[ \frac{F_1^2}{4m_N^2} + \frac{F_3^2}{16m_N^4} \right. \right. \\ & \left. \left. + \frac{F_1 F_3}{2m_N} \frac{1}{p_* \sqrt{s}} \right] \right\}, \end{aligned} \quad (1)$$

\*tulio@if.usp.br

TABLE I. Fitted parameters of the Regge model for  $\pi^0$  and  $\eta$  photoproduction from the nucleon. The fitted parameters are slightly different from our previous fitting [4] due to the correction described in Ref. [14] and the exclusion of few data points at extreme forward direction. Details are in the text.

Meson	$\gamma_1(\sqrt{\mu\text{b}})$	$\gamma_3(\sqrt{\mu\text{b}})$	$\gamma_1^{\text{cut}}(\sqrt{\mu\text{b}})$	$\gamma_3^{\text{cut}}(\frac{\sqrt{\mu\text{b}}}{\text{GeV}})$	$a(\text{GeV}^{-2})$	$\frac{\chi^2}{\text{d.o.f.}}$
$\pi^0$	127.1(14)	61.6(17)	33.88(66)	10.23(23)	0.668(12)	$\frac{110.6}{73}$
$\eta$	33.4(48)	27.8(41)	164.1(23)	3.3(21)	2.111(26)	$\frac{52.1}{41}$

where  $p_*$  is the meson momentum in the meson-nucleon center of mass frame,  $m_N$  and  $\mu$  are the nucleon and meson masses, respectively, with  $s = (k + p_1)^2$  and  $t = (k - p)^2$  the Mandelstam variables. The  $t$ -channel helicity amplitudes  $F_1 \rightarrow F_1^\rho + F_1^\omega + F_1^{\text{cut}}$  and  $F_3 \rightarrow F_3^\rho + F_3^\omega + F_3^{\text{cut}}$  and the corresponding  $\rho$  and  $\omega$  trajectories are taken from Ref. [4]. Table I summarizes the parameters of the Regge model for  $\pi^0$  and  $\eta$  photoproduction obtained by fitting the data of Figs. 1 and 2 of Ref. [4]. The fits take into account the Coulomb amplitude [4] (with the PDG recommended values [15] for  $\Gamma_{\pi^0(\eta)} \rightarrow \gamma\gamma$ ) and do not include the data points at extreme forward angles ( $|t| < 0.001 \text{ GeV}^2$  for  $\pi^0$  and  $|t| < 0.02 \text{ GeV}^2$  for  $\eta$ ) due to the effects of angular resolution neglected in our approach. Considering a  $\chi^2$  analysis, we found a constructive (destructive) interference between the Coulomb and strong amplitudes for the case of  $\pi^0(\eta)$ .

Figure 1 presents our results for  $\pi^0$  photoproduction at  $k = 5.8 \text{ GeV}$  in comparison with the data of Ref. [16]. The solid blue line represents the Regge model with the Coulomb amplitude constructively interfering with  $F_1$ , while the dashed red line includes only the strong part (assumed the same for protons and neutrons). The green dotted line represents the contribution of the  $\rho$  and  $\omega$  poles fitted in the range  $0.005 \leq |t| \leq 0.3 \text{ GeV}^2$ . The inclusion of the Regge cuts has a strong impact on the elementary cross section but a negligible effect (less than 2%) on the final results off complex nuclei mostly

due to short-range correlations for low  $t$  [17]. The Primakoff peak shown in Fig. 1 agrees with the predictions from Refs. [3,18] and is one order of magnitude higher than our previous result (see Fig. 3 from Ref. [4]) due to the correction discussed in Ref. [14]. For the case of  $\eta$  photoproduction, the absence of data for  $k \gtrsim 6 \text{ GeV}$  at extreme forward angles makes it difficult to unambiguously extract the fitted parameters with the desired accuracy. We expect that further measurements on the proton will significantly improve this deficiency [11].

The results for complex nuclei are then obtained after running the MCMC algorithm as described in Ref. [4]. Figure 2 shows our predictions for  $\pi^0$  photoproduction (solid red lines) from carbon (left) and lead (right) simultaneously scaled by a factor  $C_{\text{NI}} = 1.35 \pm 0.03$  to fit the cross section *excess* (data points) found in Ref. [3]. The *excess* is obtained by the subtraction of the coherent contribution (dashed blue lines) [3] from PrimEx data [8] and the error in  $C_{\text{NI}}$  is only statistical. The cascade results consider a meson elasticity ( $\varepsilon_{\pi^0} = \sqrt{p^2 + \mu^2}/k$ ) greater than 0.982 in accordance with [8], reproducing the data with reasonable accuracy ( $\chi^2/\text{d.o.f.} = 1.47$ ). The strong correlation between the coherent and incoherent part of the cross section influences the analysis of carbon data, since both components have almost the same magnitude at  $\theta_{\pi^0} \sim 2.2$  degrees. Also, the analysis performed by Group II from PrimEx (see Table I from

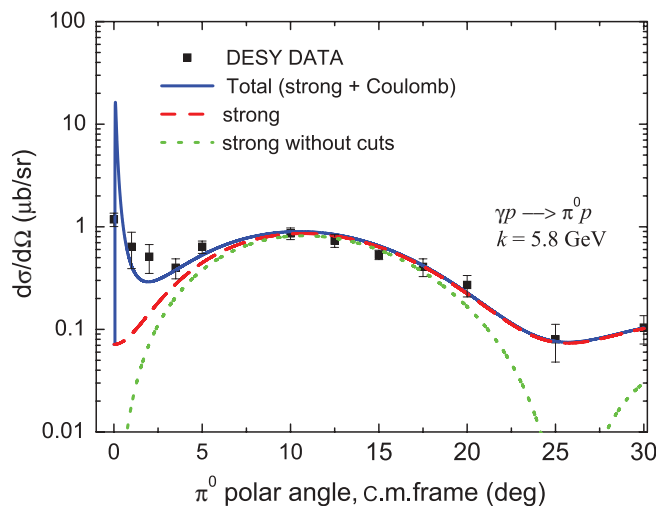


FIG. 1. (Color online) Differential cross section for  $\pi^0$  photoproduction on the proton. The first point at zero degree is omitted in the fitting due to the effects of angular resolution neglected in our analysis. Details are in the text.

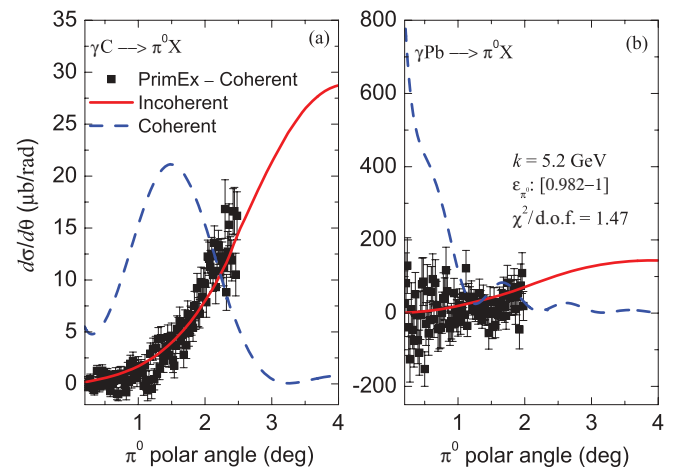


FIG. 2. (Color online) Cross section *excess* (data points) found in Ref. [3] for carbon (left) and lead (right) in comparison with the MCMC model predictions (scaled by  $1.35 \pm 0.03$ ) for the NI cross sections (solid red lines). Also shown are the results for coherent photoproduction (dashed blue lines) from Ref. [3]. Details are in the text.

Ref. [8]) found  $C_{\text{NI}} = 0.69 \pm 0.05$  for carbon when fitting the MCMC results with a slightly different pion elasticity ( $\varepsilon_{\pi^0} \geq 0.92$ ). Despite to the fact that the present analysis refers to the data from Group I [19] (Figs. 3 and 4 from [8]), we found a factor two between the fitting parameters  $C_{\text{NI}}$ , indicating that the scaling of the MCMC predictions for the NI cross section is strongly dependent on the model used for the coherent part [2,3]. Additional data at larger angles—where the coherent contribution vanishes—would provide a more stringent verification of the shape [20] and magnitude of the incoherent cross section. For the case of the lead target, the incoherent cross section is very small and the angular range of the measurements does not allow a definite conclusion about its contribution.

The calculations for  $\eta$  follow the same steps adopted for  $\pi^0$ , except for the treatment of the  $\eta$ -nucleus FSI. The latter is evaluated considering only two processes for the  $\eta N$  collisions: (i) the elastic  $\eta N \rightarrow \eta N$  scattering and, (ii) the meson absorption  $\eta N \rightarrow XN$ . The total  $\eta N$  cross section and the angular distributions for the elastic scattering are assumed to be proportional to the  $\pi^0 N$  case, such that:  $\sigma_{\eta N \rightarrow X} = C \sigma_{\pi^0 N \rightarrow X}$  and  $d\sigma_{\eta N \rightarrow \eta N} = C d\sigma_{\pi^0 N \rightarrow \pi^0 N}$ , with  $\sigma_{\pi^0 N \rightarrow X}$  and  $d\sigma_{\pi^0 N \rightarrow \pi^0 N}$  taken from Ref. [4] and  $C$  representing a scaling factor independent of meson momentum. The results for incoherent  $\eta$  photoproduction at  $k = 9$  GeV and  $C = 1$  are presented (solid red lines) in the upper panels of Fig. 3 for carbon (left) and lead (right), where we also show the predictions for the coherent part (dashed blue lines) from Ref. [3]. It is verified that for polar angles typically above 1.0 to 1.2 degrees the

incoherent processes are the most relevant mechanisms with the coherent cross sections being clearly negligible above approximately 1.5 degrees. This finding—combined with high-precision measurements at higher angles—can constrain the contribution of the inelastic backgrounds due to incoherent photoproduction also below the Coulomb peaks, which are the crucial signals for the extraction of the decay width. Furthermore, considering the differential cross sections  $\frac{d\sigma}{d\Omega}$ , the Coulomb peak angle is target independent to first order ( $\sim \frac{\mu^2}{2k^2}$ ), while the strong peak angles occur at multiples of  $\sim \frac{2}{kR}$  ( $R$  being the nuclear radius). Consequently, for heavy nuclei both components peak almost at the same angles and the extraction of the decay width via a fitting procedure becomes more challenging. For light nuclei, on the other hand, the situation is completely different and the Coulomb peak is clearly identified in Fig. 3(a). For this reason, further measurements of the  $\eta \rightarrow \gamma\gamma$  decay width via the Primakoff approach should be focused on light nuclei as they provide much higher electromagnetic responses when compared to the proton target (factor  $Z^2$ ). The lower plots of Fig. 3 represent the increase ( $\sim 20\%$  for carbon and  $\sim 55\%$  for lead) of the incoherent cross sections assuming a smaller  $\eta N$  cross section ( $C = 0.5$ ). Future measurements for heavy nuclei at larger angles—where the coherent parts are negligible—represent promising candidates to determine the unknown  $\eta N$  cross section in the medium.

In conclusion, the MCMC cascade has shown that the cross section *excess* found for carbon in Ref. [3] can be consistently assigned to the mechanism of incoherent photoproduction

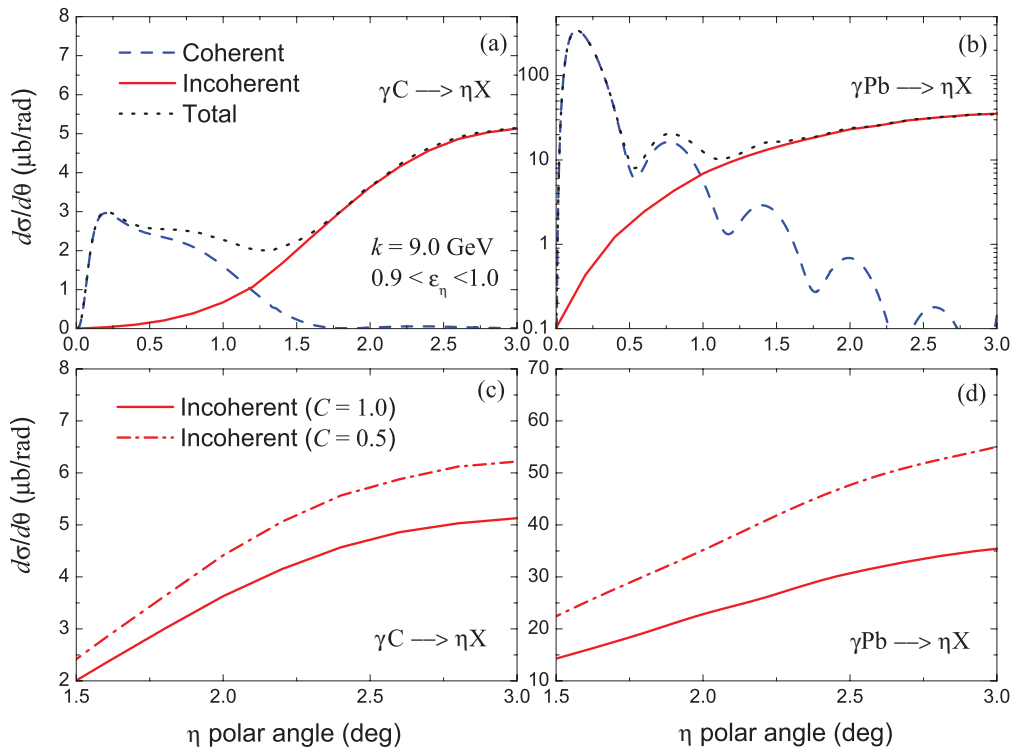


FIG. 3. (Color online) Upper panels: Differential cross section of  $\eta$  photoproduction (dotted black lines) off carbon (left) and lead (right) and the contributions from coherent (dashed blue lines) [3] and incoherent (solid red lines) photoproduction. Lower panels: NI cross sections off carbon (left) and lead (right) from MCMC model for  $\sigma_{\eta N} = \sigma_{\pi^0 N}$  (solid red) and  $\sigma_{\eta N} = 0.5\sigma_{\pi^0 N}$  (dashed red). Details are in the text.

with a fitted parameter ( $C_{\text{NI}} = 1.35 \pm 0.03$ ) a factor two higher than the value found in Ref. [8]. This result shows that the scaling of the MCMC model (NI process) with the PrimEx data at larger angles is strongly correlated with the coherent contribution [2,3]. For the case of lead, the NI cross section is very small and one should consider additional measurements at higher angles with improved statistics before any definite conclusion. Our predictions for  $\eta$  photoproduction, together with the recent results from [3], show qualitatively that future measurements of the  $\eta \rightarrow \gamma\gamma$  decay width via the Primakoff method should be focused on the proton (to accurately constrain the parameters for the

elementary amplitude) and also on light nuclei, where the Coulomb and strong parts are more easily separated [Fig. 3(a)]. The combination of the MCMC results with high precision measurements on heavy nuclei could also provide a suitable approach to access the unknown  $\eta N$  cross section in cold nuclear matter.

We would like to thank the PrimEx Collaboration for sending us their data and the Brazilian agency FAPESP for the partial support of this work. We are also indebted to Ulrich Mosel and Murat Kaskulov for useful discussions and for communicating their results on coherent photoproduction.

- 
- [1] H. Primakoff, *Phys. Rev.* **81**, 899 (1951).
  - [2] S. Gevorkyan, A. Gasparian, L. Gan, I. Larin, and M. Khandaker, *Phys. Rev. C* **80**, 055201 (2009).
  - [3] M. M. Kaskulov and U. Mosel, *Phys. Rev. C* **84**, 065206 (2011).
  - [4] T. E. Rodrigues *et al.*, *Phys. Rev. C* **82**, 024608 (2010).
  - [5] T. E. Rodrigues *et al.*, *Phys. Rev. Lett.* **101**, 012301 (2008).
  - [6] T. E. Rodrigues and J. D. T. Arruda-Neto, *Phys. Rev. C* **84**, 021601(R) (2011).
  - [7] J. S. Bell and R. Jackiw, *Nuovo Cimento A* **60**, 47 (1969); S. L. Adler, *Phys. Rev.* **177**, 2426 (1969); J. L. Goity, A. M. Bernstein, and B. R. Holstein, *Phys. Rev. D* **66**, 076014 (2002); B. Ananthanarayan and B. Moussallam, *J. High Energy Phys.* **05** (2002) 052; K. Kampf and B. Moussallam, *Phys. Rev. D* **79**, 076005 (2009); B. Ioffe and A. Oganesian, *Phys. Lett. B* **647**, 389 (2007).
  - [8] I. Larin *et al.*, *Phys. Rev. Lett.* **106**, 162303 (2011).
  - [9] R. Miskimen, *Annu. Rev. Nucl. Part. Sci.* **61**, 1 (2011).
  - [10] A. M. Bernstein and B. R. Holstein, [arXiv:1112.4809v1](https://arxiv.org/abs/1112.4809v1) [hep-ph].
  - [11] A. Gasparian *et al.*, JLab experiment no. E1210011 [[http://www.jlab.org/exp\\_prog/proposals/10prop.html](http://www.jlab.org/exp_prog/proposals/10prop.html)] (2010).
  - [12] The contribution of Regge cuts on the elementary photoproduction of pseudoscalar mesons is quite controversial and more sophisticated approaches [18,21–23] also provide accurate and interesting results. However, until more precise data at higher energies (including also polarization observables) are available, we consider the current Regge phenomenology suitable for calculations in complex nuclei; where the short-range correlations and meson-nucleus FSI are expected to play a major role [17].
  - [13] A. Gasparian and S. Gevorkyan (private communication).
  - [14] In our previous works [4,5] the longitudinal momentum transfer  $\frac{\mu^2}{2k}$  was incorrectly calculated using  $k_*$  (photon momentum in the c.m. of the  $s$  channel) instead of the correct value  $k$  (laboratory frame). This correction changes substantially the magnitude of the Coulomb peak at extreme forward directions, but has a negligible effect in the strong part of the cross sections both for  $\pi^0$  and  $\eta$  photoproduction. Since the latter work as input for the MCMC model, the results obtained for complex nuclei in the present analysis (Figs. 2 and 3) are indistinguishable from the ones presented in Refs. [4,5].
  - [15] J. Beringer *et al.* (Particle Data Group), *Phys. Rev. D* **86**, 010001 (2012).
  - [16] M. Braunschweig, W. Braunschweig, D. Husmann, K. Lübelmeyer, and D. Schmitz, *Nucl. Phys. B* **20**, 191 (1970).
  - [17] T. E. Rodrigues, J. D. T. Arruda-Neto, D. Dale, and P. Cole, in *Proceedings of the VIII Latin American Symposium on Nuclear Physics and Applications, Santiago, 2009*, Vol. 1265 (AIP, Melville, NY, 2010), p. 268.
  - [18] J. M. Laget, *Phys. Rev. C* **72**, 022202(R) (2005).
  - [19] The incoherent cross sections used by Group I in Ref. [8] are taken from S. Gevorkyan, A. Gasparian, L. Gan, I. Larin, and M. Khandaker, *Phys. Part. Nucl. Lett.* **9**, 18 (2012).
  - [20] The shape of the NI cross section for light nuclei is closely related with the mechanism of Pauli-blocking, the forward peaked elastic meson-nucleon scattering and the momentum distribution (MD) of the bound nucleons. The latter is accurately described in the MCMC cascade using  $s$ - and  $p$ -shell knock-out reactions as described in Ref. [4].
  - [21] A. Sibirtsev, J. Haidenbauer, S. Krewald, U.-G. Meißner, and A. W. Thomas, *Eur. Phys. J. A* **41**, 71 (2009).
  - [22] A. Sibirtsev, J. Haidenbauer, S. Krewald, and U.-G. Meißner, *Eur. Phys. J. A* **44**, 169 (2010).
  - [23] Jun He and B. Saghai, *Phys. Rev. C* **82**, 035206 (2010).